THE ASTROPHYSICAL JOURNAL, 853:103 (12pp), 2018 February 1 https://doi.org/10.3847/1538-4357/aaa249

"Twisting" Motions in Erupting Coronal Pseudostreamers as Evidence for Interchange Reconnection

Y.-M. Wang[1] and P. Hess
Space Science Division, Naval Research Laboratory, Washington, DC 20375, USA; yi.wang@nrl.navy.mil, phillip.hess.ctr@nrl.navy.mil
Received 2017 December 11; accepted 2017 December 14; published 2018 January 26

Abstract

Using white-light observations from the COR1 coronagraph during 2008–2013, we have identified ∼50 eruptive events in which a narrow streamer structure appears to rotate about its radial axis as it rises into the field of view beyond $r \sim 1.4\,R_\odot$. Extreme-ultraviolet images and potential-field extrapolations suggest that most of these eruptions involve one arcade of a double-lobed pseudostreamer, which is surrounded by open flux of a single polarity. The "twisting" is manifested by the cavity of the erupting lobe, which evolves from a circular to a narrowing oval structure as it is ejected nonradially in the direction of the original X-point. At the same time, the loop legs on the trailing side of the rising cavity/flux rope expand and straighten out, starting at the outer edge of the lobe and progressing inward; this asymmetric opening-up contributes to the impression of a three-dimensional structure twisting away from the observer. On the leading side of the lobe, collapsing cusps are sometimes detected, suggesting the presence of a current sheet where the cavity loops reconnect with the oppositely directed open flux from the adjacent coronal hole. In some events, the inner loops of the cavity/flux rope may continue to expand outward without undergoing interchange reconnection. The transfer of material to open field lines, as well as the lateral confinement of the pseudostreamer by the surrounding coronal holes, acts to produce a relatively narrow, fan-like ejection that differs fundamentally from the large, bubble-shaped ejections associated with helmet streamers.

Key words: Sun: activity – Sun: corona – Sun: coronal mass ejections (CMEs) – Sun: filaments, prominences – Sun: heliosphere – Sun: magnetic fields

Supporting material: animations

1. Introduction

Coronal streamers fall into two distinct categories: "helmet streamers" that separate coronal holes/open magnetic flux of opposite polarity and "pseudostreamers" that separate coronal holes of the same polarity (see, e.g., Eselevich et al. 1999; Zhao & Webb 2003; Liu 2007; Wang et al. 2007, 2012; Panasenco & Velli 2010, 2013; Crooker et al. 2012; Riley & Luhmann 2012; Yang et al. 2015). Helmet streamers (pseudostreamers) overlie an odd (even) number of photospheric neutral lines and loop arcades. Helmet streamers give rise to gradually accelerating, bubble-shaped coronal mass ejections (CMEs), whereas pseudostreamers produce narrow CMEs characterized by a fan-like structure (Wang 2015).

Panasenco et al. (2013) have described a variety of nonradial or lateral motions observed in filament eruptions underneath both types of streamers, including the rolling of the filament about its axis, which occurs very early during the eruption (see also Liewer et al. 2013). They noted that the ejected prominence material tends to propagate nonradially away from the adjacent coronal hole and toward the nearest null point. The nonradial motions of the enveloping CME are in the same sense as those of the filament but are less pronounced.

As suggested by the twin filament ejections that were observed on 2010 August 1 and described by Panasenco & Velli (2010), Török et al. (2011), and Panasenco et al. (2013), pseudostreamers may be especially prone to "sympathetic" eruptions. The MHD simulations of Török et al. (2011) and Lynch & Edmondson (2013) have shown how a current sheet may form between the rising lobe of a pseudostreamer and the open flux overlying the adjacent lobe, triggering interchange reconnection and rapidly disrupting the first lobe. The remaining lobe then erupts as it comes into contact with the "tether-cutting" current sheet trailing the first lobe. The two lobes are ejected nonradially and in opposite directions. In the Török et al. model, each lobe initially contains a flux rope, and the first current sheet forms after a neighboring eruption compresses the pseudostreamer; as interchange reconnection weakens the field overlying the far lobe, the flux rope inside it is ejected via the torus instability (Kliem & Török 2006). In the 2.5D simulation of Lynch & Edmondson (2013), each lobe consists of an ordinary loop arcade, and the reconnection and breakout process is initiated by shearing the footpoints of one of the arcades.

Evidence for interchange reconnection during a pseudostreamer eruption has been presented by Yang et al. (2015). In this event, observed on 2012 September 9 with the Atmospheric Imaging Assembly on the *Solar Dynamics Observatory*, a filament located under one lobe of a pseudostreamer was ejected toward the coronal hole adjacent to the other lobe. In addition to a double-ribbon brightening underneath the disrupted lobe, a ribbon-like brightening appeared along the edge of the remote hole, consistent with the conversion of some of its open flux into closed loops by interchange reconnection.

The COR1 coronagraphs on the *Solar Terrestrial Relations Observatory* (*STEREO*) *A* and *B* spacecraft have a field of view extending over the heliocentric range $r \sim 1.4$–$4\,R_\odot$. While recently examining running-difference movies in the COR1 CME catalog maintained by Hong Xie,[2] we came across a remarkable class of events in which a narrow streamer structure rises above the COR1 occulter and appears to rotate slowly about its stalk. Because the streamer structure usually contains

[1] NRC Research Associate.

[2] See https://cor1.gsfc.nasa.gov.

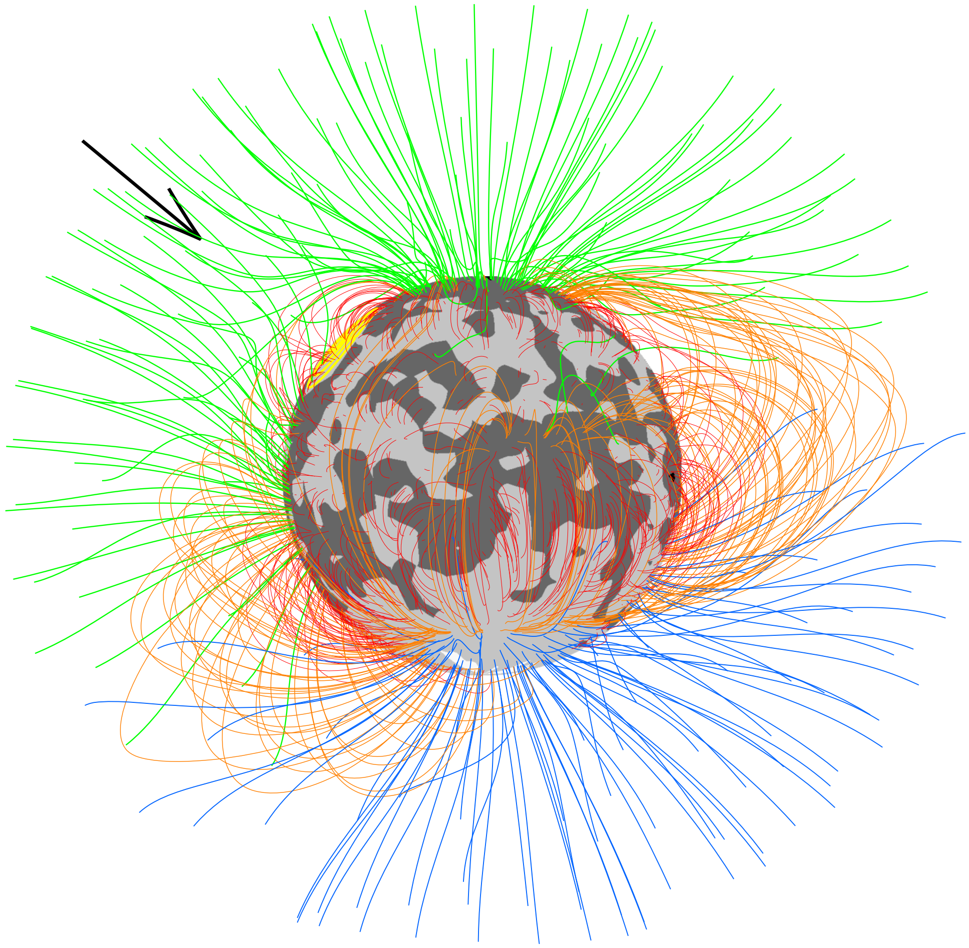

Figure 1. Coronal field-line configuration on 2008 April 12 (00:00 UTC), as viewed from *STEREO-B*. The black arrow points to the double-lobed pseudostreamer that produced successive eruptions during April 10–14, with its footpoint area at the northeast limb being shaded yellow. The coronal field was derived by applying a PFSS extrapolation (with source surface at $r = R_{ss} = 2.5\,R_\odot$) to an NSO map of the radially oriented photospheric field, B_r, during CR 2068. Open field lines having negative (positive) polarity are coded green (blue); closed loops are orange if they extend beyond $r = 1.5\,R_\odot$, red otherwise. Black, dark gray, light gray, and white denote areas of the photosphere where $B_r < -6$ G, -6 G $< B_r < 0$ G, 0 G $< B_r < +6$ G, and $B_r > +6$ G, respectively. The pseudostreamer (at latitude $L \sim +40°$) is surrounded by negative-polarity open flux originating from coronal holes at the north pole and near the equator.

a concave-outward core or cavity, the catalog tags these events with a comment such as "narrow FR rises." From comparisons with the underlying structure observed with the *STEREO* Extreme UltraViolet Imager (EUVI) and from potential-field source-surface (PFSS) extrapolations, we inferred that the great majority of the "twisting" structures were pseudostreamers. During the interval 2008–2013, we identified ∼50 such events, some of which were observed from different angles by both *STEREO-A* and *STEREO-B*.

In this paper, we describe a selection of COR1 events that illustrate the quasi-twisting motions of erupting pseudostreamers, and we present a physical interpretation of this striking phenomenon.

2. Data Processing

The *STEREO* COR1-A/B coronagraphs, deployed since 2006, provide white-light observations of the inner corona down to $r \sim 1.4\,R_\odot$ (see Thompson et al. 2003; Howard et al. 2008). COR1 data are recorded in three-image polarized sequences, which we combine into single total-brightness images with a typical cadence of 5 minutes. To reduce the instrumental noise, we then add four successive images to obtain 20-minute averages. Running-difference images and movies are constructed by subtracting from a given averaged one image taken roughly an hour earlier.

To track ejecta beyond $r \sim 4\,R_\odot$, we employ white-light observations from *STEREO* COR2-A/B, whose field of view extends from ∼4 to ∼15 $R_\odot$.

Height–time maps are constructed by extracting radial strips, centered at a given position angle (PA), from COR1 and COR2 running-difference images, and arranging the double row of strips in a time-ordered sequence. Here, the COR1 data were not averaged in time.

Running-difference, undifferenced, base-ratio, and/or sharpened images from *STEREO* EUVI-A/B, taken primarily in Fe XII 19.5 nm and He II 30.4 nm, are used to relate the coronagraph observations to the underlying source regions below $r \sim 1.4\,R_\odot$.

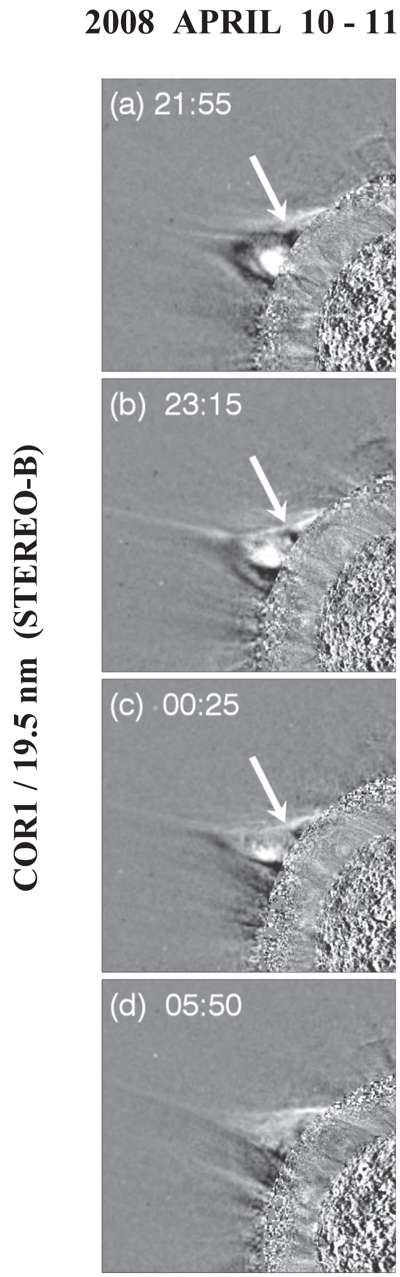

Figure 2. Sequence of composite COR1/EUVI-B running-difference images showing the pseudostreamer eruption of 2008 April 10–11. (a) The lower-latitude lobe of the pseudostreamer rises into the COR1 field of view above $r \sim 1.4\ R_\odot$ (April 10, 21:55 UTC). The adjacent higher-latitude lobe is visible in Fe XII 19.5 nm. (b) The core/cavity of the lobe has emerged fully into the COR1 field, exhibiting the concave-outward topology of a flux rope (April 10, 23:15 UTC). (c) The cavity seems to twist in the poleward direction, as its poleward side erodes away (April 11, 00:25 UTC). (d) The cavity is no longer visible (April 11, 05:50 UTC). The arrows in (a)–(c) point to small, cusp-shaped features that appear to be collapsing onto the top of the higher-latitude lobe (see the accompanying movie). Here and in subsequent figures, north is up and west is to the right.

(An animation of this figure is available.)

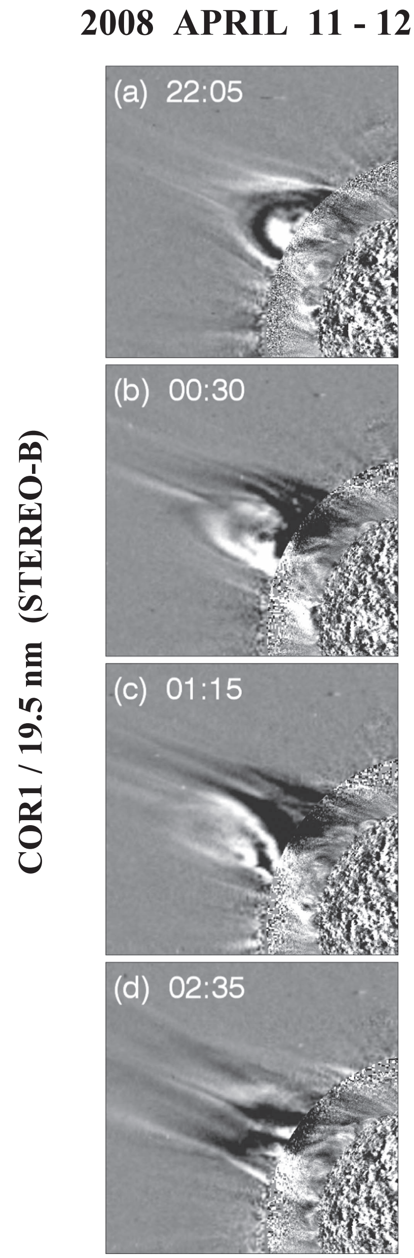

Figure 3. Sequence of composite COR1/EUVI-B running-difference images showing the higher-latitude lobe of the pseudostreamer erupting during 2008 April 11–12. In this case, the cavity appears to twist equatorward, not poleward as in Figure 2. This impression is at least partly due to the outward expansion of the loop legs on the poleward (trailing) side of the cavity, starting at the outer edge of the lobe and proceeding inward ((a)–(c)). By 02:35 UTC on April 12, the cavity has seemingly been converted into a collection of ray-like features (d).

(An animation of this figure is available.)

3. Serial Eruptions of a Pseudostreamer Near Solar Minimum

During 2008 April 10–14, as sunspot activity approached its minimum, COR1-B recorded a succession of small eruptions from a double-lobed pseudostreamer above the northeast limb. Figure 1 displays the coronal field-line configuration as viewed from *STEREO-B* on April 12; the arrow indicates the location of the pseudostreamer, which is surrounded on its poleward and equatorward sides by open flux of negative polarity. The coronal field was derived by applying a PFSS extrapolation, with the field constrained to become radial at $r = R_{ss} = 2.5\ R_\odot$, to photospheric flux measurements recorded by the National Solar Observatory (NSO) during Carrington rotation (CR) 2068.

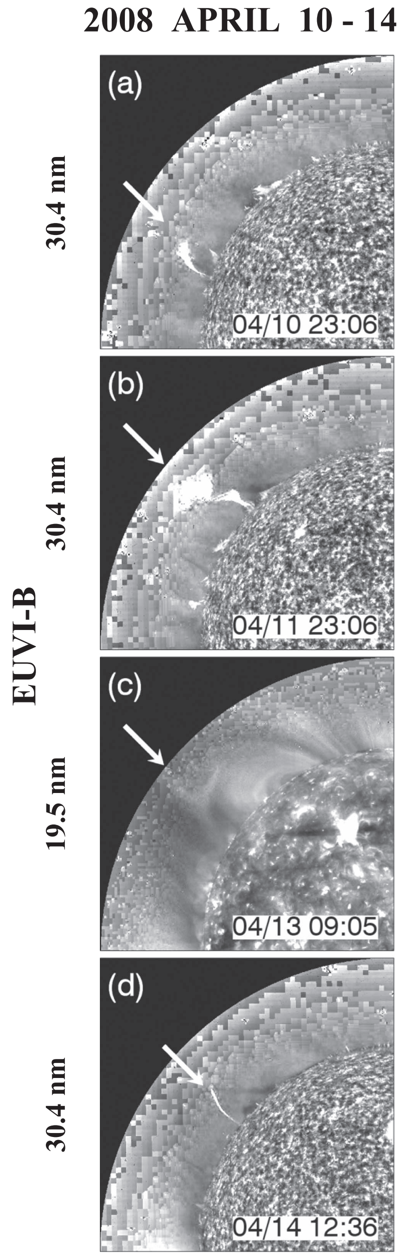

Figure 4. EUVI-B running-difference images showing four successive filament eruptions under the pseudostreamer of Figures 1–3 during 2008 April 10–14. (a) At 23:06 UTC on April 10, a He II 30.4 nm filament is ejected poleward from the lower-latitude arcade of the pseudostreamer, giving rise to the white-light event of Figure 2. (b) At 23:06 UTC on April 11, a 30.4 nm filament is ejected equatorward from the higher-latitude arcade of the pseudostreamer, triggering the white-light event of Figure 3. (c) At 09:05 UTC on April 13, a V-shaped flux rope seen in Fe XII 19.5 nm is ejected poleward from the lower-latitude lobe. (d) At 12:36 UTC on April 14, a small 30.4 nm filament is ejected poleward, again from the lower-latitude lobe. The last two eruptions gave rise to faint white-light events in which the pseudostreamer lobe appeared to twist in the poleward direction (see the COR1 CME catalog).

The first eruption is shown by the composite COR1/EUVI images in Figure 2. On April 10, the lower-latitude lobe of the pseudostreamer emerges into the COR1 field (Figure 2(a)). The stationary higher-latitude lobe is visible in Fe XII 19.5 nm, while its apex may be seen protruding above the COR1 occulter. The core/cavity of the rising lobe, which takes on the form of a concave-outward flux rope, progressively narrows (Figures 2(b)–(c)), disappearing from view by 05:50 UTC on April 11 (Figure 2(d)). The impression given by the accompanying running-difference movie is that the axis of the cavity, initially pointing toward the observer, rotates poleward toward the sky plane, as the poleward edge of the cavity erodes away. The arrows in Figures 2(a)–(c) indicate the locations of small, cusp-shaped features that seem to be collapsing onto the top of the higher-latitude lobe (see the animation).

Late on April 11, the large higher-latitude lobe of the pseudostreamer erupts (Figure 3). Again, the initially circular cavity becomes increasingly elongated, eventually being transformed into a collection of radial rays. The linear features first appear at the poleward edge of the lobe, where they evidently represent the legs of highly stretched loops (Figure 3(a)); they then spread toward the center of the cavity, which begins to take the form of a V-shaped flux rope as the loop legs pinch inward (Figures 3(b)–(c)). Meanwhile, the leading/equatorward side of the lobe gradually erodes away. As the loop legs on the trailing side straighten out, the entire cavity/flux rope seems to disappear (Figure 3(d)). The sequence of running-difference images in Figure 3 and the accompanying movie give the impression that the axis of the cavity rotates equatorward toward the sky plane, not poleward as in the first event (Figure 2).

The EUVI-B images in Figure 4 focus on the structures underlying the pseudostreamer and their evolution during April 10–14. The COR1 event of Figure 2 is associated with a filament eruption observed in He II 30.4 nm at 23:06 UTC on April 10 (Figure 4(a)). The filament originates from inside the lower-latitude arcade and is ejected in the poleward direction. Approximately a day later, the filament underlying the higher-latitude arcade is ejected in the equatorward direction (Figure 4(b)); this eruption corresponds to the COR1 event of Figure 3. Early on April 13, the lower-latitude lobe erupts again; the 19.5 nm image in Figure 4(c) shows a V-shaped structure being ejected poleward. In the COR1 CME catalog, a corresponding white-light event (much narrower and fainter than the preceding one in Figure 3) may be seen, in which the axis of the pseudostreamer appears to twist in the poleward direction. On April 14, another filament is ejected poleward from the same lower-latitude arcade (Figure 4(d)); the COR1 CME catalog again shows a narrow, poleward-twisting pseudostreamer lobe.

4. Sympathetic Eruptions in Pseudostreamers

The three ejections from alternating lobes of the pseudostreamer during 2008 April 10–13 provide support for the idea that the pseudostreamer topology tends to promote sympathetic eruptions (Panasenco & Velli 2010; Török et al. 2011; Lynch & Edmondson 2013). Further examples of pairs of sympathetic eruptions from pseudostreamers are displayed in the composite EUVI/COR1 images in Figure 5 (for movies of some of these events, see the COR1 CME catalog).

The EUVI-A image in Figure 5(a), recorded at 11:46 UTC on 2008 June 10, shows a He II 30.4 nm filament being ejected in the equatorward direction from the higher-latitude lobe of a pseudostreamer above the northeast limb. A corresponding white-light CME may be seen in the COR1-A image, whose cavity appears to rotate equatorward about the pseudostreamer stalk (compare Figure 3). At 17:36 UTC on June 11, a filament

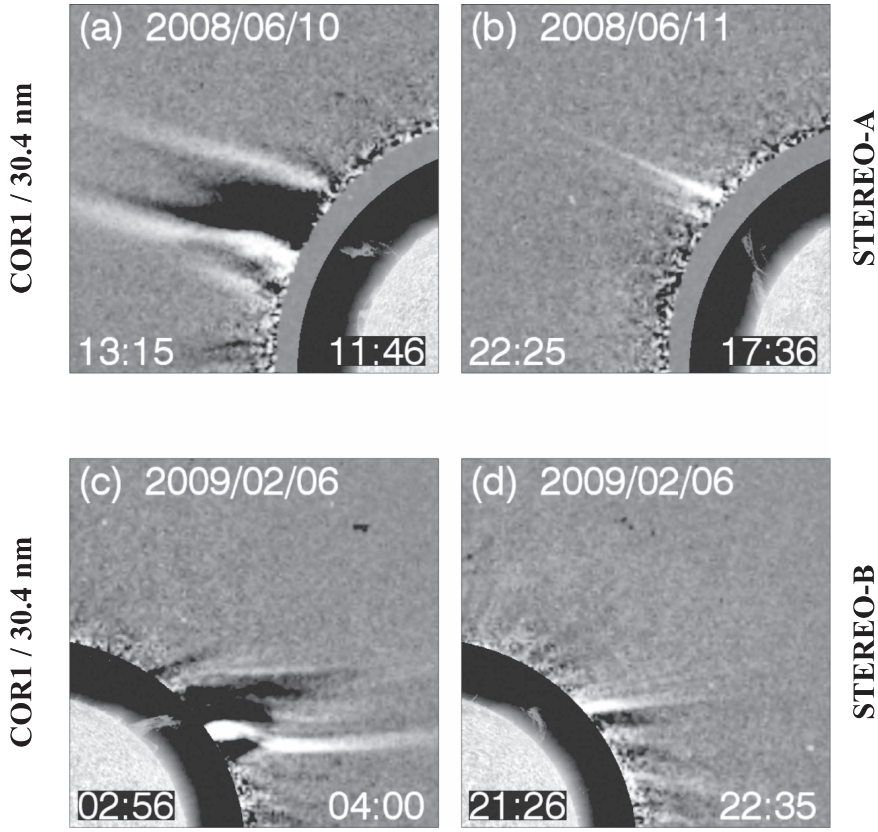

Figure 5. Composite COR1/EUVI images showing further examples of sympathetic eruptions from pseudostreamers. (a) At 11:46 UTC on 2008 June 10, *STEREO-A* observes a He II 30.4 nm filament being ejected equatorward from inside the higher-latitude lobe of a pseudostreamer at the northeast limb. As suggested by the COR1 running-difference image taken at 13:15 UTC, the erupting lobe appears to twist equatorward (a movie of this event may be found in the COR1 CME catalog). (b) At 17:36 UTC on June 11, a filament is ejected in the poleward direction from the lower-latitude lobe of the same pseudostreamer. The narrow white-light structure seen at 22:25 UTC is in the process of twisting poleward. (c) At 02:56 UTC on 2009 February 6, *STEREO-B* observes a 30.4 nm filament being ejected equatorward from inside the higher-latitude lobe of a pseudostreamer at the northwest limb. The erupting white-light lobe, here shown at 04:00 UTC, appears to twist equatorward (a movie may be found in the COR1 CME catalog). (d) At 21:26 UTC on the same day, a filament is ejected poleward from the lower-latitude lobe of the pseudostreamer. The faint white-light structure seen at 22:35 UTC seems to twist poleward.

is ejected in the poleward direction from the lower-latitude lobe of the same pseudostreamer (Figure 5(b)). The white-light image shows a narrow structure that seems to twist in the poleward direction.

In the EUVI-B image in Figure 5(c), recorded at 02:56 UTC on 2009 February 6, a filament is ejected equatorward from the higher-latitude lobe of a pseudostreamer above the northwest limb. As expected, the COR1 counterpart "rolls" toward the equator. A poleward-directed filament ejection from the lower-latitude lobe is observed at 21:26 UTC on the same day (Figure 5(d)). Correspondingly, the narrow structure seen in the COR1 image seems to twist poleward.

The examples shown in Figures 2–5 suggest a tendency for poleward-directed ejections to produce weaker white-light events than equatorward-directed ones. One factor that may contribute to this asymmetry is the presence of relatively strong polar fields near solar minimum, with the poleward gradient in the magnetic pressure acting to oppose changes in the high-latitude coronal structure.

Although sympathetic eruptions from alternating lobes appear to be relatively common in pseudostreamers, many of the eruptions that we observed during 2008–2013 (including those discussed in the following sections) were not immediately preceded or followed by a clearly identifiable ejection from the other lobe.

5. "Twisting" Pseudostreamers Viewed from Opposite Directions: Incompatibility with Rotation

If the observed "twisting" of the erupting pseudostreamer lobe represents an actual rotation, the sense of the rotation about the radial axis should remain the same (either clockwise or counterclockwise) when viewed from different longitudes. During 2011–2012, many pseudostreamer events were observed simultaneously by COR1-A and -B from widely separated angles.

As an illustrative example, Figure 6 shows the poleward lobe of a pseudostreamer erupting during 2011 May 25, as viewed from *STEREO-A* (left panels) and from *STEREO-B* (right panels), at a longitudinal separation of 173° from *-A*. The pseudostreamer is located above the northeast (northwest) limb as seen from A (B), with the two spacecraft looking in opposite directions along a line of sight that coincides roughly with the axis of the lobe arcade. As it rises, the white-light cavity elongates and appears to twist equatorward, as seen by both COR1-A and COR1-B. However, if this apparent twist were interpreted as a rotation about the pseudostreamer stalk, the sense of rotation (as defined looking down along the axis) would be opposite for the two spacecraft: clockwise for an observer at A, but counterclockwise for an observer at B. As discussed in the next section, the impression of equatorward twisting comes mainly from the expansion and

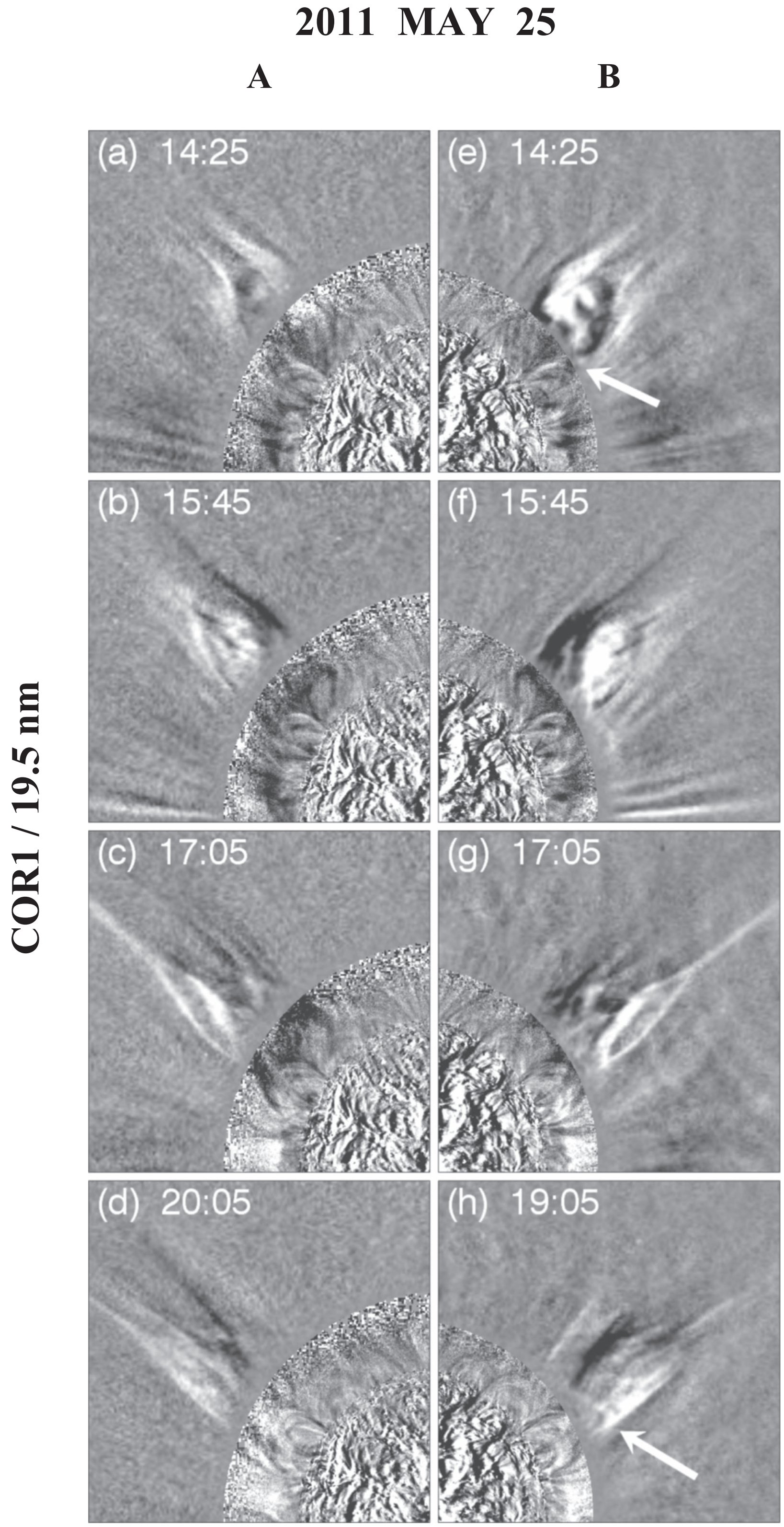

Figure 6. Comparison of *STEREO-A* (left column) and *STEREO-B* (right column) views of a pseudostreamer eruption on 2011 May 25. From both perspectives, separated by 173° in longitude, the higher-latitude lobe of the pseudostreamer appears to twist toward the equator, as the loop legs on its poleward side expand outward and the cavity progressively narrows. If the "twist" were an actual rotation about the pseudostreamer stalk, the rotation would have opposite senses as seen from the two spacecraft. The arrows in the COR1-B images recorded at 14:25 and 19:05 UTC point to cusp-shaped features collapsing onto the lower-latitude lobe of the pseudostreamer (visible in the underlying 19.5 nm images).

(An animation of this figure is available.)

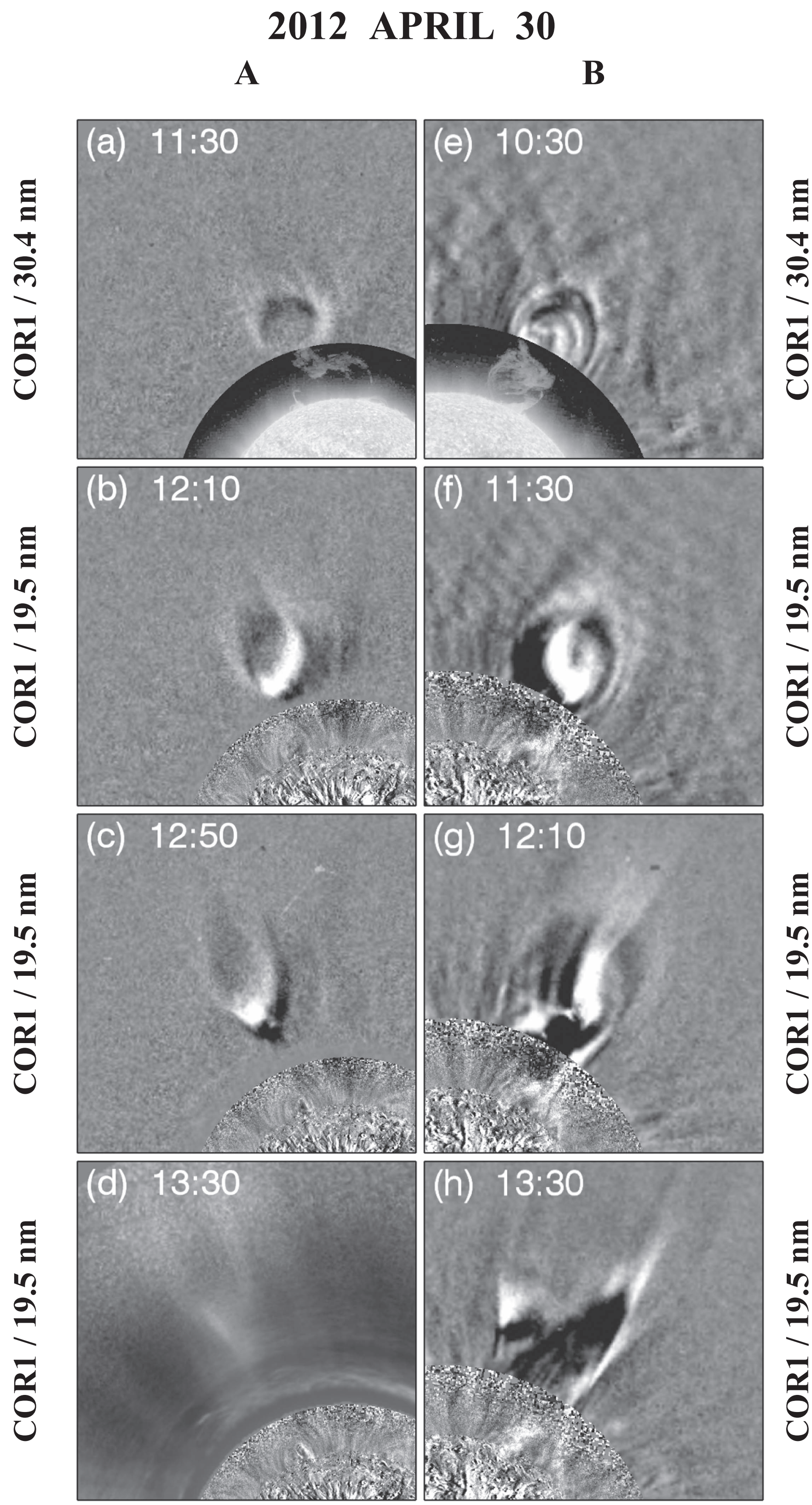

Figure 7. Eruption of the higher-latitude lobe of a pseudostreamer on 2012 April 30, as viewed from *STEREO-A* (left column) and from *STEREO-B* (right column), at a longitudinal separation of 128° from *-A*. Again, the lobe appears to twist equatorward from both viewing angles, as the loop legs expand on the trailing/poleward side. The COR1-A observations, including the undifferenced image in (d), show that the core of the lobe survives in the form of a V-shaped flux rope (see also Figure 11(f) below).

(An animation of this figure is available.)

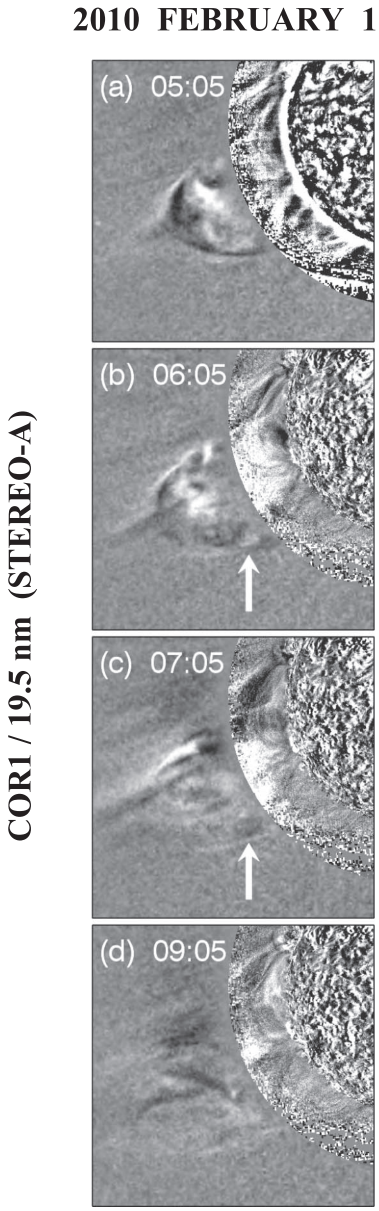

Figure 8. Sequence of composite COR1/EUVI-A images showing the lower-latitude lobe of a pseudostreamer erupting above the southeast limb on 2010 February 11. The cavity appears to twist poleward as it rises above the COR1 occulter. The arrows point to inward-moving, cusp-like features at the poleward edge of the lobe (see the accompanying movie). The cusps collapse onto the higher-latitude lobe of the pseudostreamer, visible in the Fe XII 19.5 nm images.

(An animation of this figure is available.)

straightening of the loop legs on the trailing side of the lobe, accompanied by a progressive narrowing of the cavity.

In the COR1-B images recorded at 14:25 and 19:05 UTC (Figures 6(e) and (h)), the arrows indicate the location of faint inflows along the leading edge of the erupting lobe, which may be seen in the animation accompanying Figure 6. These cusp-like features are directed toward the top of the non-erupting, lower-latitude arcade of the pseudostreamer (visible in Fe XII 19.5 nm).

As another example, the *STEREO-A* and *-B* images of Figure 7 show the poleward lobe of a pseudostreamer erupting on 2012 April 30, when the two spacecraft were separated by 128°. From both perspectives, the cavity appears to twist equatorward as the arcade loops rise and pinch inward; again, this is inconsistent with actual rotation about a radial axis. In the COR1-B images, the higher-latitude or trailing side of the cavity is converted into an array of long, curved features. The COR1-A images show clearly that the remnant of the cavity has the form of a narrow, V-shaped flux rope.

Similar results were found by comparing the COR1-A and -B views of pseudostreamer eruptions on 2011 February 11, April 28, May 13, July 14, November 5, and December 9 (see the A and B movies for these events in the COR1 CME catalog).

These comparisons suggest that the apparent rotational motion is an illusion caused by the intrinsic structural evolution of the pseudostreamer lobe and its motion in the sky plane (see Section 6). Indeed, the white-light data alone do not allow us to distinguish between rotation toward or away from the observer. For the same reason, we cannot rule out the possibility that actual rotational motions (such as those associated with the conversion of twist into writhe) may be present in pseudostreamer eruptions.

6. Factors That Contribute to the Impression of Rotation

A number of effects combine to give the illusion of twisting by the erupting pseudostreamer lobe. As it drifts in the equatorward or poleward direction, the cavity becomes progressively narrower, resembling a circular disk that is initially seen face-on but gradually turns away from the observer. In addition, the conversion of the trailing side of the lobe into a succession of long, curved features, starting at its outer edge and proceeding toward the center of the cavity, gives the impression of a three-dimensional cylindrical structure whose axis is initially along the line of sight but progressively swings in the leading direction. As demonstrated in the preceding section, however, this apparent rotation of the cavity axis does not have a unique sense when viewed from opposite directions along the line of sight.

7. Evidence for Inflows Associated with Pseudostreamer Eruptions

As described in Hess & Wang (2017), we have recently identified large numbers of inflows below $r \sim 2\,R_\odot$ using the COR1 coronagraph. The great majority of these collapsing features are observed in the aftermath of helmet streamer eruptions and are localized near the base of the ray-like structures/current sheets that trail the ejected flux ropes.

Among the ~50 pseudostreamer events that we examined for the present study, we were able to detect inflows in only a small number of cases, including the eruptions of 2008 April 10–11 (Figure 2) and 2011 May 25 (Figure 6). Two additional events that show clear evidence for inflows are displayed in Figures 8 and 9.

In the composite COR1/EUVI-A images of Figure 8, the lower-latitude lobe of a pseudostreamer is seen erupting above the southeast limb on 2010 February 11. As it rises through the COR1 field of view, the cavity seems to twist in the poleward direction. The arrows point to the location of cusp-like features on the poleward side of the cavity, which appear to be collapsing onto the higher-latitude lobe of the pseudostreamer (see the accompanying animation).

Half a rotation later, on 2010 February 24, the lower-latitude lobe of the same pseudostreamer undergoes another eruption

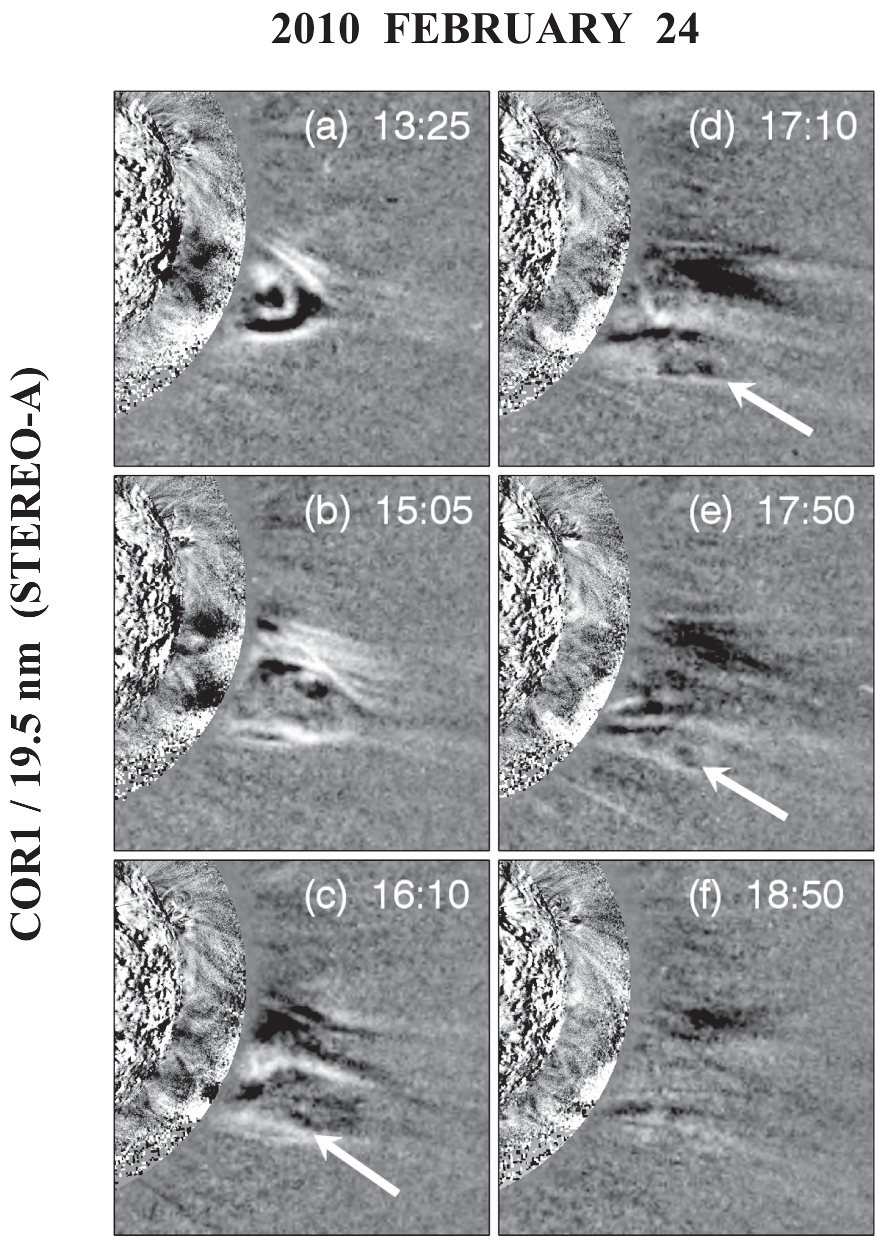

Figure 9. Sequence of composite COR1/EUVI-A images showing the lower-latitude lobe of the pseudostreamer of Figure 8 erupting again on 2010 February 24, when the pseudostreamer has rotated to the southwest limb. As the loop legs on its equatorward side expand outward, the lobe appears to twist poleward. The arrows indicate the locations of small features that collapse along the leading edge of the lobe (see the accompanying movie).

(An animation of this figure is available.)

above the southwest limb (Figure 9). Again, small inward-moving features are observed along the poleward edge of the poleward-twisting cavity (see the animation accompanying Figure 9).

In all four cases, the inflows are localized on the side of the disrupted lobe that leads in the direction of its nonradial motion, which is also the side adjacent to the vertical separatrix of the pseudostreamer. It is along this interface that the cavity loops are expected to encounter open flux of the opposite polarity, leading to the formation of a current sheet (see, e.g., Török et al. 2011; Lynch & Edmondson 2013).

It is unclear to us whether the absence of conspicuous inflows in the majority of our pseudostreamer events is a real effect or whether it is due to the low sensitivity of the COR1 instrument. However, the relatively subtle nature of the collapsing features that we have so far been able to detect suggests that more may be present at or below the noise level.

8. Origin of the Asymmetry in the Erupting Lobe

Our analysis so far has suggested that the twisting of the pseudostreamer about its radial axis is an illusion due to the progressive narrowing of the cavity and the asymmetric evolution of its two sides.

To understand physically how this asymmetry arises, we note that the erupting lobe has a velocity component directed toward the vertical separatrix of the pseudostreamer, which divides the two arcades and the like-polarity coronal holes on either side. Along this boundary, the leading edge of the lobe is compressed as it runs into open flux of the opposite polarity,

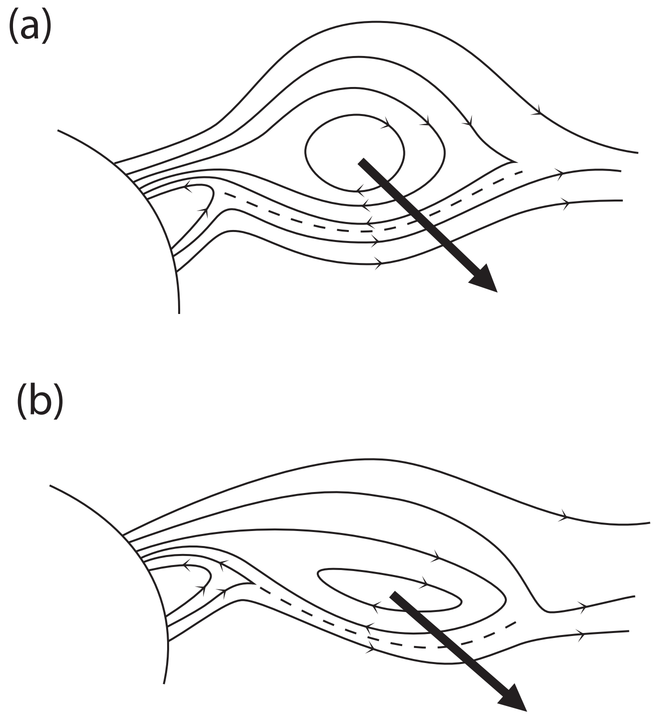

Figure 10. Asymmetric evolution of an erupting pseudostreamer lobe due to interchange reconnection. (a) The higher-latitude lobe is ejected equatorward, and a current sheet (dashed line) forms where it runs into the oppositely directed open flux rooted on the equatorward side of the pseudostreamer. (b) Reconnection at the current sheet transfers open flux to the trailing side of the lobe, while producing pinched-off loops that collapse onto the lower-latitude lobe of the pseudostreamer. As the erupting lobe elongates in the radial direction, its equatorward side progressively erodes away.

and a current sheet is expected to form. As indicated by the COR1 observations, the loops rooted on the trailing side of the lobe expand and begin to open up during the early stages of the eruption. The remnant of the cavity, which continually elongates in the radial direction and develops a V-shaped bottom, becomes localized near the leading edge of the lobe; in some cases, it eventually disappears from view or is completely transformed into ray-like features.

Reconnection between open and closed flux at the current sheet that forms at the leading edge provides a simple explanation for the asymmetric evolution of the pseudostreamer lobe. The interchange process would convert the loop legs rooted on the trailing side of the lobe into open field lines, while producing collapsing loops on the leading side (see Figure 10). This scenario is supported by the observations of cusp-like features collapsing onto the non-erupting lobe of the pseudostreamer (Figures 2, 6, and 8–9), as well as by the MHD simulations mentioned earlier.

As noted above, however, we have detected collapsing cusps at the leading edge of the lobe in only a handful of events. If the absence of inflows in the majority of cases is real and not (as we suspect) a result of visibility effects, the implication would be that interchange reconnection proceeds too slowly to convert most of the cavity loops into open flux. Both legs of the loops would then continue to expand outward, perhaps driven by the torus instability. The observed asymmetry might be attributed to the effect of ram pressure alone, which opposes the lateral expansion of the loops at the leading edge of the lobe but not on its trailing side.

In general, however, both interchange reconnection and confinement by ram pressure are likely to contribute to the asymmetrical evolution of the lobe, with the interchange process helping to drive the eruption by stripping away some of the overlying loops (see, e.g., the simulation of Török et al. 2011).

9. Pseudostreamer Ejections in the Outer Corona

The COR2 images in Figure 11 show the extensions beyond $r \sim 4\ R_\odot$ of some of the previously described COR1 ejections. In the events of 2008 April 12, 2008 June 10, 2010 February 11, 24, and 2011 May 25, the CME has a simple fan-like structure. However, the CME of 2012 April 30 is dominated by a V-shaped flux rope containing dense filament material, as is the corresponding COR1-A ejection in Figure 7. If the ray-like morphology of the first five events is attributed to the effect of interchange reconnection, then the interchange process has only partially converted the cavity field into open flux in the last event. In all cases, the ejections have relatively small angular widths, ranging from $\sim 20°$ to $\sim 30°$.

Figure 12 displays composite COR1/COR2 height–time maps for the events of 2008 April 12, 2011 May 25, and 2012 April 30. In each case, two kinds of COR1 tracks may be distinguished: nearly flat tracks with slopes corresponding to speeds of $\sim$10–30 km s^{-1}; and, diverging from them, tracks that curve steeply upward and merge with their COR2 counterparts. The speeds remain roughly constant beyond $r \sim 4\ R_\odot$ and are typically in the range $\sim$250–450 km s^{-1}.

The flat COR1 tracks (which eventually steepen) may be identified with the slowly rising pseudostreamer cavity/flux rope. At least some of the faint, steep tracks may represent material released from the trailing side of the lobe by interchange reconnection.

10. Summary and Conclusions

During 2008–2013, the *STEREO*/COR1 coronagraph recorded at least 50 events in which a narrow streamer structure rose above $r \sim 1.4\ R_\odot$ and appeared to rotate about its vertical axis. EUVI images as well as PFSS extrapolations indicate that the erupting structures represent one lobe of a pseudostreamer. The occurrence rate of these events was greater during 2008–2011, when the polar coronal holes were present, than during the subsequent period of polar field reversal. This, and the tendency for the eruptions to occur at mid-latitudes, can be explained by the fact that pseudostreamers are often located between the polar holes and lower-latitude holes of the same polarity. Analysis of some of the best-observed events leads to the following conclusions.

1. In accordance with earlier observational (e.g., Panasenco et al. 2013) and theoretical (Török et al. 2011; Zuccarello et al. 2012; Lynch & Edmondson 2013) studies, the erupting pseudostreamer lobe generally has a nonradial velocity component directed toward the adjacent lobe.
2. Several of the pseudostreamer events were preceded or followed within a day by an eruption from the other lobe (see Figures 2–5). In these sympathetic eruptions, the filaments in the two adjacent lobes were ejected in opposite directions toward the original X-point, as predicted in the simulations of Török et al. (2011) and Lynch & Edmondson (2013).
3. If the higher-latitude lobe of a pseudostreamer erupts, its poleward/trailing side appears to twist toward the observer (see, e.g., Figure 3). Equivalently, the arcade

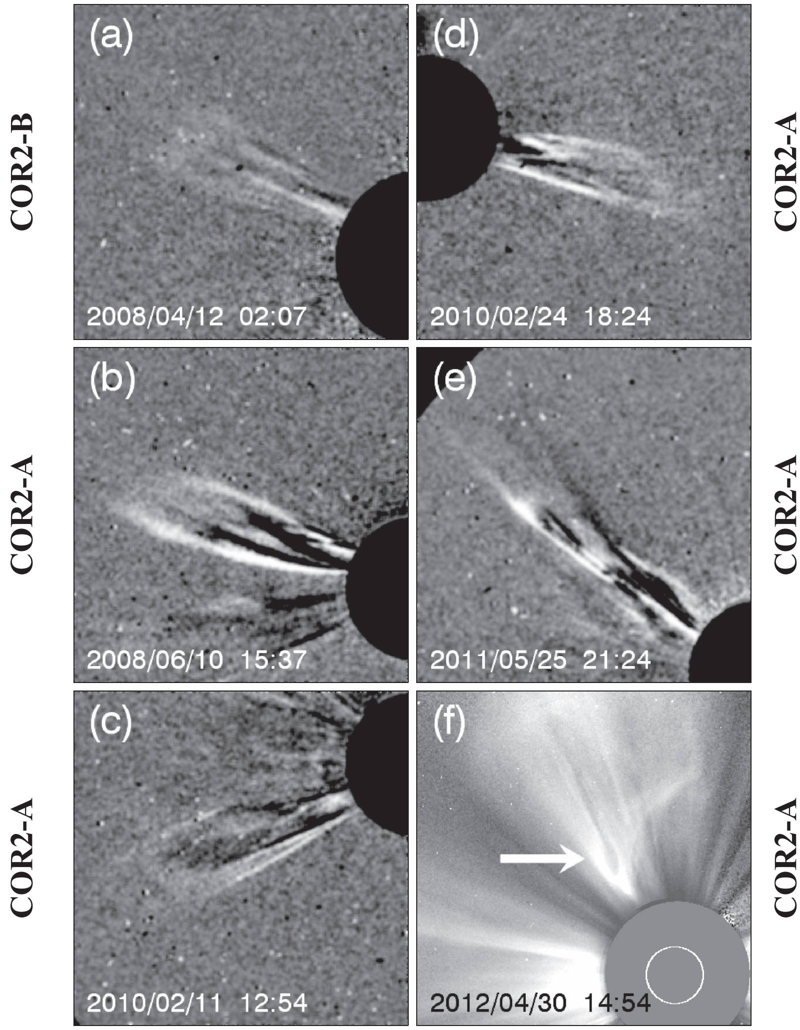

Figure 11. Extensions of some of the previously described pseudostreamer ejections into the COR2 field beyond $r \sim 4\,R_\odot$. (a) 2008 April 12, 02:07 UTC (COR2-B; compare Figure 3). (b) 2008 June 10, 15:37 UTC (COR2-A; compare Figure 5(a)). (c) 2010 February 11, 12:54 UTC (COR2-A; compare Figure 8). (d) 2010 February 24, 18:24 UTC (COR2-A; compare Figure 9). (e) 2011 May 25, 21:24 UTC (COR2-A; compare Figure 6, left column). (f) 2012 April 30, 14:54 UTC (COR2-A; compare Figure 7, left column). The ejections are characterized by a fan- or jet-like morphology, with angular widths of only ~20°–30°. However, as indicated by the arrow in the undifferenced image in (f), the 2012 April 30 CME also contains a prominent V-shaped flux rope.

axis (initially perpendicular to the sky plane) seems to rotate equatorward toward the sky plane, with the circular cavity becoming progressively more oval-shaped. If the lower-latitude lobe erupts, its equatorward/trailing side appears to twist toward the observer (the arcade axis seems to rotate poleward: see, e.g., Figure 2).

4. In those cases where COR1-A and -B view the same event from opposite directions (as in Figures 6 and 7), both see the trailing side of the lobe twisting toward it. This is inconsistent with actual rotation about a radial axis.
5. The impression that the erupting lobe is turning about its radial axis is due to its translational motion and morphological evolution. As it drifts equatorward or poleward, the initially circular cavity evolves into an oval-shaped structure (like a face-on disk that gradually turns away from the observer). In addition, the two sides of the lobe evolve asymmetrically, with the loops expanding rapidly on the trailing side but being compressed and/or pinching off on the leading side. The progressive transformation of the trailing loop legs into a series of rays gives the illusion of a three-dimensional structure twisting in the leading direction.
6. The COR1 running-difference movies accompanying Figures 2, 6, and 8–9 show small, cusp-shaped features collapsing onto the top of the non-erupting lobe of the pseudostreamer. The probable source of these inflows is interchange reconnection occurring where the rising lobe encounters the oppositely directed open flux above the adjacent lobe.
7. Interchange reconnection at the leading edge of the lobe provides a natural explanation for the sequential opening-up of loops on the trailing side and for the progressive erosion of the leading side (Figure 10). Although the

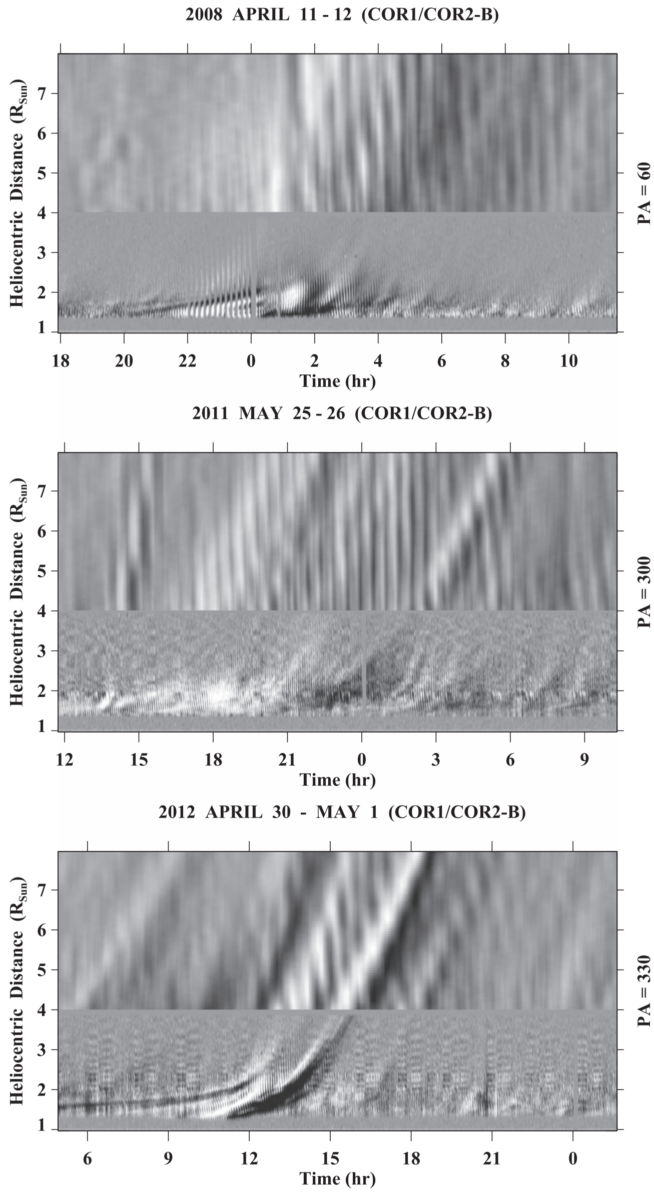

Figure 12. Height–time maps constructed from COR1/COR2-B running-difference images. (a) 2008 April 11–12 (PA = 60°). (b) 2011 May 25–26 (PA = 300°). (c) 2012 April 30–May 1 (PA = 330°). At least two kinds of tracks may be distinguished: (1) low, flat tracks produced by the slowly rising pseudostreamer cavities, and, curving steeply upward from them, (2) fainter tracks produced by the escaping loop material. The ejecta reach relatively constant speeds of ∼250–450 km s^{-1} in the COR2 field of view beyond $r \sim 4\,R_\odot$.

expected inflows are visible in only a few events, many of these faint features may have been missed because of the high noise level of the COR1 instrument.

8. In some cases, not all of the arcade loops are stripped away and converted into open flux, but the cavity survives as a V-shaped flux rope (see Figures 7(d) and 11(f)).
9. As observed beyond $r \sim 4\,R_\odot$, pseudostreamer CMEs tend to have a fan- or jet-like morphology, widths of only ∼20°–30°, and roughly constant speeds (Figures 11–12; see also Wang 2015). Their linear structure and narrow widths may be attributed both to the effect of lateral confinement by the surrounding unipolar open flux and to the transfer of their material from closed loops to the adjacent coronal-hole field lines by interchange reconnection.

It is evident that pseudostreamers tend to produce ejections that are smaller and weaker than the CMEs associated with helmet streamers. The basic reason for this difference is that, in pseudostreamers, the overlying field falls off relatively slowly, with the like-polarity open flux from the surrounding coronal holes converging above the X-point and acting to confine the erupting lobe both laterally and in the radial direction. By stripping away at least some of the overlying field, interchange reconnection helps to drive the eruption and may act to trigger the torus instability (Török et al. 2011). The actual amount of reconnection that takes place may depend on the strength of the underlying driver. Thus, an active region flare (see Figure 5(d) in Wang 2015) would inject far more energy into a pseudostreamer lobe than a small filament eruption, causing the core field to expand impulsively while undergoing less interchange reconnection with the neighboring coronal hole. In the case of helmet streamers, the loops underlying the Y-point have a natural tendency to expand in both the radial and transverse directions, leading to much larger, bubble-shaped eruptions.

We thank B. Kliem and D.G. Socker for helpful discussions. This work was supported by the NASA H-GI Program and by the Chief of Naval Research.

ORCID iDs

Y.-M. Wang https://orcid.org/0000-0002-3527-5958

References

Crooker, N. U., Antiochos, S. K., Zhao, X., & Neugebauer, M. 2012, JGR, 117, A04104
Eselevich, V. G., Fainshtein, V. G., & Rudenko, G. V. 1999, SoPh, 188, 277
Hess, P., & Wang, Y.-M. 2017, ApJ, 850, 6
Howard, R. A., Moses, J. D., Vourlidas, A., et al. 2008, SSRv, 136, 67
Kliem, B., & Török, T. 2006, PhRvL, 96, 255002
Liewer, P. C., Panasenco, O., & Hall, J. R. 2013, SoPh, 282, 201
Liu, Y. 2007, ApJL, 654, L171
Lynch, B. J., & Edmondson, J. K. 2013, ApJ, 764, 87
Panasenco, O., Martin, S. F., Velli, M., & Vourlidas, A. 2013, SoPh, 287, 391
Panasenco, O., & Velli, M. 2010, in AGU Fall Meeting, Abstr. SH51A-1663 (Washington, DC: AGU)
Panasenco, O., & Velli, M. 2013, in AIP Conf. Proc. 1539, Solar Wind 13, ed. G. P. Zank et al. (Melville, NY: AIP), 50
Riley, P., & Luhmann, J. G. 2012, SoPh, 277, 355
Thompson, W. T., Davila, J. M., Fisher, R. R., et al. 2003, Proc. SPIE, 4853, 1
Török, T., Panasenco, O., Titov, V. S., et al. 2011, ApJL, 739, L63
Wang, Y.-M. 2015, ApJL, 803, L12
Wang, Y.-M., Grappin, R., Robbrecht, E., & Sheeley, N. R., Jr. 2012, ApJ, 749, 182
Wang, Y.-M., Sheeley, N. R., Jr., & Rich, N. B. 2007, ApJ, 658, 1340
Yang, J., Jiang, Y., Xu, Z., Bi, Y., & Hong, J. 2015, ApJ, 803, 68
Zhao, X. P., & Webb, D. F. 2003, JGR, 108, 1234
Zuccarello, F. P., Bemporad, A., Jacobs, C., et al. 2012, ApJ, 744, 66